Inorg. Chem. **1988**, *27*, 2185–2189 **2185**

Contribution from the Department of Chemistry, Gorlaeus Laboratories, Leiden University, P.O. Box 9502,
2300 RA Leiden, The Netherlands, and School of Chemical Sciences, National Institute for Higher Education, Dublin 9, Ireland

Synthesis and Spectroscopic and Electrochemical Properties of Mononuclear and Dinuclear Bis(2,2′-bipyridyl)ruthenium Complexes Containing 3,5-Bis(pyridin-2-yl)-1,2,4-triazole

Ronald Hage,[†] Anouk H. J. Dijkhuis,[†] Jaap G. Haasnoot,[*,†] Rob Prins,[†] Jan Reedijk,[†]
Barbara E. Buchanan,[‡] and Johannes G. Vos[‡]

Received November 4, 1987

The compounds $[Ru(bpy)_2(bpt)]^+$ and $[(Ru(bpy)_2)_2(bpt)]^{3+}$, where Hbpt = 3,5-bis(pyridin-2-yl)-1,2,4-triazole and bpy = 2,2′-bipyridyl, have been prepared as PF_6^- salts and have been characterized. ^1H NMR spectra obtained for the dinuclear compound suggest that two different geometrical isomers are obtained. By the use of NMR spectroscopy, an attempt was made to identify the structure of these species. A distinct shift in the electronic spectra was observed when the coordinated bpt ligand was protonated. For both the mono- and dinuclear compounds, an emission was observed at room temperature. The pK_a values of the free ligand, the mononuclear compound, and the binuclear compound are 8.4, 4.0, and –0.6, respectively. For the dinuclear compound, two redox potentials were observed for the ruthenium-based oxidation with a difference of 0.32 V. Also for the dinuclear compound, a strong metal–metal interaction was observed, indicated by a large value for the electron delocalization α^2 (9.4×10^{-3}). This was confirmed by the small solvent dependence of this transition.

Introduction

Considerable attention has been paid to the studies of ruthenium compounds containing 2,2′-bipyridine (bpy) because of their potential application as catalysts for the photochemical cleavage of water.[1–6] Especially, dinuclear ruthenium compounds have attracted much attention, not only because of their ability to transfer two electrons but also because of the present interest in mixed-valence compounds.[7–30] Studies on these dinuclear compounds have concentrated on these mixed-valence compounds, and their physical properties have been discussed in the light of models published by Hush.[28,29] In particular, the intervalence transition (IT) of the mixed-valence compounds has been studied extensively, as its position, shape, and intensity yield information about the interaction between the metal centers. Other points of interest are the electrochemical and excited-state properties of these compounds.[15,30]

In a previous paper, we reported the properties of a series of mononuclear $Ru(bpy)_2$ complexes containing various pyridyltriazoles (Rpyrtr).[31] In the present work, the synthesis and characterization of mono- and dinuclear $Ru(bpy)_2$ complexes with 3,5-bis(pyridin-2-yl)-1,2,4-triazole (Hbpt; see Figure 1) are presented. The compounds obtained have been investigated by using NMR, UV/vis, and emission spectroscopy and electrochemical techniques. The pH dependence of the spectroscopic and electrochemical data has also been studied to obtain more information about the properties of the mononuclear and dinuclear compounds.

Experimental Section

Materials. 3,5-Bis(pyridin-2-yl)-1,2,4-triazole (Hbpt) was prepared according to literature methods.[34] ^1H NMR [$(CD_3)_2SO$]: 8.67 (d, H6), 8.15 (d, H3), 8.00 (t, H4), 7.52 ppm (t, H5). ^{13}C NMR: 158.9 (C3′), 149.7 (C6), 147.7 (C2), 137.4 (C4), 124.6 (C5), 122.1 ppm (C3).

The mononuclear compound, $[Ru(bpy)_2(bpt)](PF_6)$, containing anionic bpt, was prepared by refluxing 1 mmol of $Ru(bpy)_2Cl_2(H_2O)_2$[35] and 1.2 mmol of Hbpt in 50 mL of $EtOH/H_2O$ (2:1) for 6 h. The hot solution was filtered and evaporated until dryness, after which 10 mL of water was added to the dark red product. The compound was precipitated by adding an excess of aqueous NH_4PF_6 to the solution. After filtration, the compound was purified by column chromatography, with neutral alumina and ethanol as eluent. Further purification took place by recrystallization from water/acetone (1:1). Anal. Calcd for $[Ru(bpy)_2(bpt)]PF_6{\cdot}H_2O$: C, 48.12; H, 3.38; N, 15.78; P, 3.88. Found: C, 48.38; H, 3.36; N, 16.14; P, 3.46.

The dinuclear compound, $[(Ru(bpy)_2)_2(bpt)](PF_6)_3$, was prepared in a similar manner, except that 2.2 mmol of $Ru(bpy)_2Cl_2(H_2O)_2$ and 1 mmol of Hbpt in 50 mL of ethanol/water were used in reflux. After column chromatography and careful recrystallization from acetone/alcohol (2:1), two different fractions were obtained (ratio 1:1). Anal. Calcd for $[(Ru(bpy)_2)_2(bpt)](PF_6)_3$ C, 42.09; H, 2.72; N, 12.26; P, 6.27.

Table I. ^1H and ^{13}C NMR Data for $[Ru(bpy)_2(bpt)]^+$, Measured in Acetone-d_6 (Chemical Shifts in ppm Relative to TMS)

^1H NMR Data

	H3	H4	H5	H6
bpt ligand	8.44 (d)	8.23 (t)	7.41 (t)	7.66 (d)[a]
	7.20 (d)	7.9–8.2	7.27 (t)	8.23 (d)[b]
bpy ligands	8.7–8.85	7.9–8.2	7.4–7.6	7.9–8.2

^{13}C NMR Data

	bpt ligand		bpy ligands
C2	156.9–157.3	149.0	156.9–157.3
C3	120.8	122.6	123.6–124.2
C4	136.4–137.8		136.4–137.8
C5	126.7	124.5	127.3–127.6
C6	152.2	150.6	150.6–151.3
C3′	161.5	164.6	

[a] Ruthenium-bound pyridine ring of bpt. [b] Free pyridine ring of bpt.

[†] Leiden University.

[‡] NIHE.

(1) Seddon, E. A.; Seddon, K. R. *The Chemistry of Ruthenium*; Elsevier: Amsterdam, 1984.
(2) Meyer, T. J. *Acc. Chem. Res.* **1978**, *11*, 94.
(3) Meyer, T. J. *Pure Appl. Chem.* **1986**, *58*, 1193.
(4) Kalyanasanduram, K. *Coord. Chem. Rev.* **1982**, *46*, 159.
(5) Kalyanasanduram, K.; Grätzel, M.; Pelizetti, E. *Coord. Chem. Rev.* **1986**, *69*, 57.
(6) Kalyanasanduram, K.; Kiwi, J.; Grätzel, M. *Helv. Chim. Acta* **1978**, *61*, 2720.
(7) Geselowitz, D. A.; Kutner, W.; Meyer, T. J. *Inorg. Chem.* **1986**, *25*, 2015.
(8) Gilbert, J. A.; Eggleston, D. S.; Murphy, W. R.; Geselowitz, D. A.; Gersten, S. W.; Hodgson, D. J.; Meyer, T. J. *J. Am. Chem. Soc.* **1985**, *107*, 3855.
(9) Vining, W. J.; Meyer, T. J. *Inorg. Chem.* **1986**, *25*, 2023.
(10) Calvin, M. *Science (Washington, D.C.)* **1974**, *184*, 375.
(11) Dose, E. V.; Wilson, L. J. *Inorg. Chem.* **1978**, *17*, 2660.
(12) Sedney, D.; Ludi, A. *Inorg. Chim. Acta* **1981**, *47*, 153.
(13) Tinnemans, A. H. A.; Timmer, K.; Reinten, M.; Kraaijkamp, J. G.; Alberts, A. H.; van der Linden, J. G. M.; Schmitz, J. E. J.; Saaman, A. A. *Inorg. Chem.* **1981**, *20*, 3698.
(14) (a) Rillema, D. P.; Callahan, R. W.; Mack, K. B. *Inorg. Chem.* **1982**, *21*, 2589. (b) Rillema, D. P.; Mack, K. B. *Inorg. Chem.* **1982**, *21*, 3849.
(15) Braunstein, C. H.; Baker, A. D.; Strekas, T. C.; Gafney, H. D. *Inorg. Chem.* **1984**, *23*, 857.
(16) Goldsby, K. A.; Meyer, T. J. *Inorg. Chem.* **1984**, *23*, 3002.
(17) Curtis, J. C.; Bernstein, J. S.; Meyer, T. J. *Inorg. Chem.* **1985**, *24*, 385.
(18) Woitellier, S.; Launay, J. P.; Sowinska, M. *Nouv. J. Chim.* **1986**, *10*, 241.
(19) Ernst, S.; Kasack, V.; Bessenbacher, C.; Kaim, W. *Z. Naturforsch., B: Anorg. Chem., Org. Chem.* **1987**, *42B*, 425.
(20) Jaradat, Q.; Baraquawi, K.; Akasheh, T. S. *Inorg. Chim. Acta* **1986**, *116*, 63.

0020-1669/88/1327-2185$01.50/0

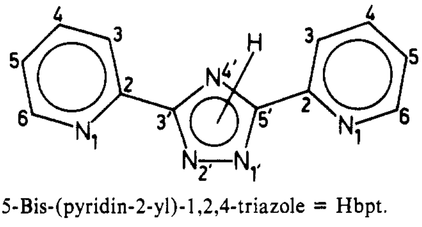

Figure 1. 3,5-Bis-(pyridin-2-yl)-1,2,4-triazole = Hbpt.

Found (fraction 1): C, 42.07; H, 2.45; N, 12.04; P, 6.65. Found (fraction 2): C, 41.86; H, 2.84; N, 12.00; P, 6.45.

The partially oxidized dinuclear compounds were not isolated but were generated in solution by chemical oxidation using $(NH_4)_2Ce(NO_3)_6$.

pK_a measurements were carried out in a Britton–Robinson buffer (0.04 M boric acid, 0.04 M acetic acid, and 0.04 M phosphoric acid); the pH of the solutions was adjusted by using 1.0 M NaOH solutions. To facilitate dissolution of the monomer in aqueous solutions, the dichloride salt was used to determine the pK_a value.

Physical Measurements. UV–vis absorption spectra were recorded on a Perkin-Elmer 330 spectrophotometer using 1-cm^3 quartz cells. Emission spectra were recorded on a Perkin-Elmer LS-5 luminescence spectrometer, equipped with a red-sensitive Hamamatsu R928 detector. Emission wavelengths are not corrected for photomultiplier response.

Proton NMR spectra were obtained either on a JEOL JNM-FX 200-MHz or on a Bruker 300-MHz spectrometer. ^{13}C NMR spectra were obtained on a JEOL JNM-FX 50.1-MHz spectrometer. All measurements have been carried out in acetone-d_6. The peak positions are relative to TMS. For the COSY experiments 256 FID's of eight scans each, consisting of 1K data points, were accumulated. After digital filtering (sine-bell squared), the FID was zero filled to 512 W in the F_1 dimension. Acquisition parameters were $F_1 = \pm$ 500 Hz, F_2 = 1000 Hz, and $t_{1/2}$ = 0.001 sec; the recycle delay was 1.5 s.

Electrochemical measurements were carried out with an EG&G Par 174A polarographic analyzer and an EG&G Par 175 universal programmer. A saturated calomel electrode (SCE) was used as the reference electrode. Measurements were carried out in spectroscopic grade CH_3CN dried over molecular sieves and with 0.1 mol dm^{-3} NEt_4ClO_4 or NBu_4ClO_4 as a supporting electrolyte. Glassy-carbon electrodes were used as working electrodes. The scan rate used was 100 mV s^{-1}. Elemental analyses were carried out at University College, Dublin.

Results and Discussion

^1H NMR Spectroscopy. Mononuclear Compound 1. The ^1H and ^{13}C NMR spectral data obtained for the mononuclear compound with bpt are listed in Table I. No complete assignment could be made, but by comparison with literature data, the major part of the spectrum could be understood.[31-33,36,39-42] Chemical shifts of the protons and carbon atoms of the pyridine ring that is coordinated to ruthenium are noticeably different from those observed for the noncoordinating pyridine ring of bpt. This is especially clear for H3. This is caused by the changes in electron density of the ruthenium-bound pyridine ring and by the steric effects between the protons of bpt and the bipyridine rings of the $Ru(bpy)_2$ moiety. This steric interaction is less when $Ru(bpy)_2$ is bound via N1′ and N1 than when it is bound via N4′ and N1.

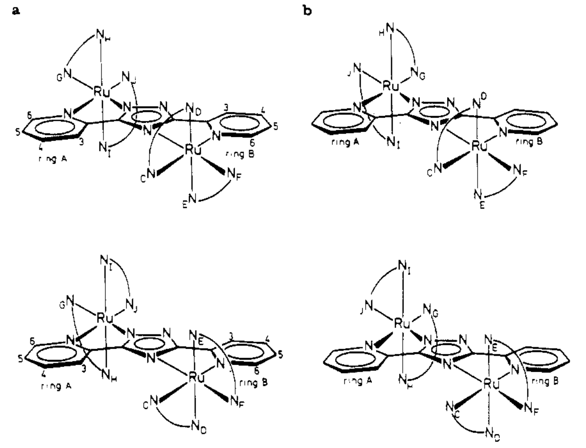

Figure 2. Proposed molecular structures of the four isomers of $[(Ru(bpy)_2)_2(bpt)]^{3+}$: (a) the two optical isomers present in fraction I (isomer **2-I**); (b) the other set of two optical isomers present in fraction II (isomer **2-II**).

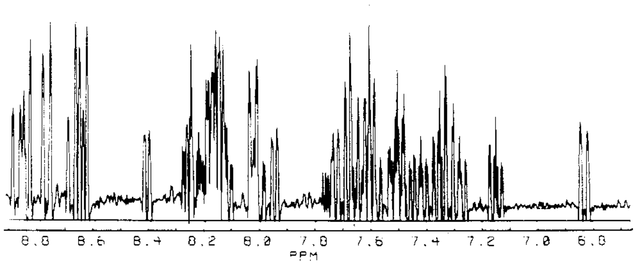

Figure 3. ^1H NMR spectrum of $[(Ru(bpy)_2)_2(bpt)]^{3+}$, isomer **2-II**. (The NMR spectrum of isomer **2-I** is presented in Figure 4.)

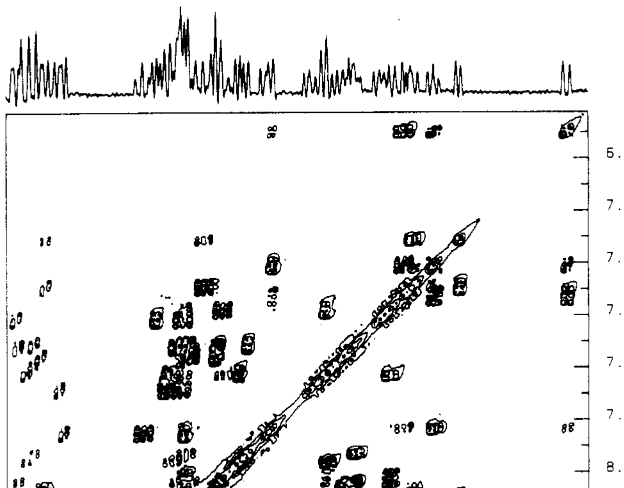

Figure 4. COSY spectrum of isomer **2-I** of $[(Ru(bpy)_2)_2(bpt)]^{3+}$, in acetone-$d_6$ at 300 MHz. For further details see the Experimental Section.

---

(21) Kober, E. M.; Goldsby, K. A.; Narayana, D. N. S.; Meyer, T. J. *J. Am. Chem. Soc.* **1983**, *105*, 4303.
(22) Sullivan, B. P.; Curtis, J. C.; Kober, E. M.; Meyer, T. J. *Nouv. J. Chim.* **1980**, *4*, 643.
(23) Sullivan, B. P.; Meyer, T. J. *Inorg. Chem.* **1980**, *19*, 752.
(24) Meyer, T. J. *Chem. Phys. Lett.* **1979**, *64*, 417.
(25) Powers, M. J.; Meyer, T. J. *Inorg. Chem.* **1978**, *17*, 1785.
(26) Callahan, R. W.; Keene, F. R.; Meyer, T. J.; Salmon, D. J. *J. Am. Chem. Soc.* **1977**, *99*, 1064.
(27) Powers, M. J.; Callahan, R. W.; Salmon, D. J.; Meyer, T. J. *Inorg. Chem.* **1976**, *15*, 894.
(28) Hush, N. S. *Prog. Inorg. Chem.* **1967**, *8*, 391.
(29) Hush, N. S. *Electrochem. Acta* **1968**, *13*, 1005.
(30) Sahai, R.; Baucom, D. A.; Rillema, D. P. *Inorg. Chem.* **1986**, *25*, 3843.
(31) Hage, R.; Prins, R.; Haasnoot, J. G.; Reedijk, J.; Vos, J. G. *J. Chem. Soc., Dalton Trans.* **1987**, 1389.
(32) Steel, P. J.; Lahousse, F.; Lerner, D.; Marzin, C. *Inorg. Chem.* **1983**, *22*, 1488.
(33) Hage, R.; Haasnoot, J. G.; Reedijk, J.; Vos, J. G. *Inorg. Chim. Acta* **1986**, *118*, 73.
(34) Geldard, J. F.; Lions, F. *J. Org. Chem.* **1965**, *30*, 318.
(35) Sullivan, B. P.; Salmon, D. J.; Meyer, T. J. *Inorg. Chem.* **1978**, *17*, 3334.
(36) Lytle, F. E.; Petrosky, L. M.; Carlson, L. R. *Anal. Chim. Acta* **1971**, *57*, 239.
(37) Kelly, J. M.; Long, C.; O'Connell, C. M.; Vos, J. G.; Tinnemans, A. H. A. *Inorg. Chem.* **1983**, *22*, 2818.
(38) Belser, P.; von Zelewsky, A. *Helv. Chim. Acta* **1980**, *63*, 1675.
(39) Walsh, J. L.; Durhan, B. *Inorg. Chem.* **1982**, *21*, 329.
(40) Cook, M. J.; Lewis, A. P.; McAuliffe, G. S. G.; Thomson, A. J. *Inorg. Chim. Acta* **1982**, *64*, L25.
(41) Creutz, C. *Prog. Inorg. Chem.* **1983**, *30*, 1.
(42) Hupp, J. T.; Meyer, T. J. *Inorg. Chem.* **1987**, *26*, 2332.

Table II. ^1H NMR Data for the Two Isomers of $[(Ru(bpy)_2)_2(bpt)]^{3+}$, Measured in Acetone-$d_6$ (Chemical Shifts in ppm Relative to TMS)

	H3	H4	H5	H6
		Isomer **2-I**		
bpt ligand	6.69	7.33	7.21	7.82
	7.11	7.29	8.08	8.73
bpy ligands	8.62	8.33	7.85	8.17
	8.81	8.18	7.52	7.92
	8.81	8.18	7.52	8.27
	8.77	8.23	7.62	7.95
	8.77	8.23	7.52	8.05
	8.72	8.14	7.56	8.10
	8.74	8.14	7.63	8.03
	8.65	8.18	7.41	8.27
		Isomer **2-II**		
bpt ligand	6.83	7.35	7.15	7.73
	7.27	7.71	8.18	8.67
bpy ligands	8.83	8.18	7.60	8.42
	8.89	8.21	7.67	8.27
	8.6–8.9	8.0–8.3	7.2–7.5	8.0–8.3

Because of the similarities between **1** and $[Ru(bpy)_2(LL')]^+$[31] (LL′ = deprotonated 3-(pyridin-2-yl)-1,2,4-triazole and 5-methyl-3-(pyridin-2-yl)-1,2,4-triazole), it was concluded that not much steric interaction is present in this compound. It is therefore likely that coordination via N1′ and N1 of bpt takes place.

Dinuclear Compound 2. The dinuclear compound may exist in two geometrical isomers depending on the relative orientation of the bipyridine rings (see Figure 2). NMR spectroscopy was found to be a useful technique in the investigation of the structure of two structural isomers of $Ru(LL')_3X_2$ compounds (LL′ is an asymmetric bidentate ligand).[32,33] To gain more information about the structure of the isomers obtained for the dinuclear complex, the ruthenium compounds reported here have been investigated by using proton NMR spectroscopy. NMR spectra of the two fractions (I and II) of the dinuclear compound are presented in Figures 3 and 4. Major steric interactions between the $Ru(bpy)_2$ moieties prevents a configuration in which the two $Ru(bpy)_2$ moieties are coordinated via N1′ and N2′, respectively, of the triazole ring, assuming a bpt conformation with pyridine rings A and B in a cis orientation. Therefore, only the two geometrical isomers, each with an optical pendant, as depicted in Figure 2 are assumed to be formed. The proton NMR spectrum obtained for fraction I (see Experimental Section) is shown in Figure 4, while the NMR spectrum of the second fraction is presented in Figure 3. Space-filling models reveal that because of the short distance between H3 of the bpt ligand and one of the bipyridine rings (ring C in Figure 2a), a large diamagnetic anisotropic interaction should occur, resulting in a shift of the resonance of H3 to higher field.[36] This effect is expected to be even more pronounced than the diamagnetic anisotropic interaction between H6 and the pyridine rings found in $Ru(bpy)_3X_2$.[36] Therefore, this proton assigned to the doublet with the lowest ppm value (6.69 ppm of isomer **2-I** and 6.83 ppm of isomer **2-II**). In Figure 4, a COSY spectrum of fraction I is presented. Despite the complexity of the spectrum, an almost complete assignment was made. On the basis of the assignment of 6.69 ppm to H3 of ring A, the COSY spectrum easily permitted the assignment of the remaining protons of this ring (see Table II). Because of the large distance to any other pyridine ring, the H3 proton of bpt pyridine ring B has neither a diamagnetic anisotropic interaction with a pyridine ring nor any steric hindrance from neighboring hydrogen atoms. Therefore, this proton will have a different chemical shift compared to those of the H3 protons of ring A of the bpt ligand and the bipyridine ligands (Table II and Figure 2). The COSY experiments did yield eight different sets of pyridine protons, each of which could be assigned to individual hydrogen atoms of the rings by comparison with the reported assignment of $[Ru(bpy)_3]X_2$.[36] It proved however not possible to assign these groups to specific bipyridyl groups. Due to the complexity of the ^1H NMR spectrum of isomer **2-II**, a less detailed analysis was made. It is clear that the same kind of interactions are present in this system.

Table III. Electronic and Electrochemical Data for $[Ru(bpy)_2(bpt)]^+$, $[Ru(bpy)_2(Hbpt)]^{2+}$, $[(Ru(bpy)_2)_2(bpt)]^{3+}$, and $[(Ru(bpy)_2)_2(Hbpt)]^{4+}$

		emission		oxidn potentials,[e] V	
compd	absorption[a] $d\pi \rightarrow \pi^*$	300 K[b]	77 K[c]	$E_{1/2}(1)$	$E_{1/2}(2)$
$[Ru(bpy)_2(bpt)]^+$	475 (1.13)	650	624	0.87	
$[Ru(bpy)_2(Hbpt)]^{2+}$	429 (1.56)	636	612	1.00	
$[(Ru(bpy)_2)_2(bpt)]^{3+}$	452 (2.26)	625	600	1.08	1.40
$[(Ru(bpy)_2)_2(Hbpt)]^{4+}$ (isomer **2-I**)	434 (2.35)	*d*		0.89	1.10
$[(Ru(bpy)_2)_2(bpt)]^{3+}$	451 (2.19)	625	600		
$[(Ru(bpy)_2)_2(Hbpt)]^{4+}$ (isomer **2-II**)	434 (2.31)	*d*			

[a] λ_{max} values are in nm; ϵ values in parentheses are in 10^4 M^{-1} cm^{-1}. [b] Measured in Britton–Robinson buffer. [c] Measured in ethanol. [d] Emission not observed for the protonated dimer. [e] Measured in CH_3CN with 0.1 M NEt_4ClO_4. Volts versus SCE.

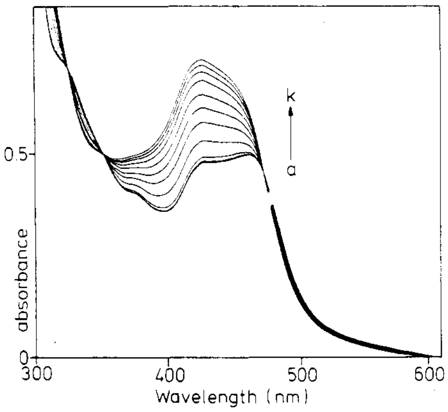

Figure 5. pH dependence of the absorption spectrum of $[Ru(bpy)_2(Hbpt)]^{2+}$ in an aqueous Britton–Robinson buffer. Curves a–k: pH 6.80, 6.16, 5.50, 4.78, 4.34, 4.09, 3.83, 3.47, 3.15, 2.73, and 1.99.

It can be shown that in isomer **2-II** the bipyridine ligands IJ and EF are more or less coplanar, whereas in isomer **2-I** this coplanarity does not exist. Because of the moderate steric interactions between the H6 protons of the coplanar bipyridine ligands in the plane, a shift to higher ppm values is expected. Normally, a chemical shift of the H6 protons in ruthenium polypyridyl systems of about 7.8 ppm is observed.[31–33,36]

Fraction II shows a remarkable doublet at about 8.4 ppm. This resonance has been assigned to a H6 proton of ring I or ring E (Figure 2b). Therefore, it is likely that the bipyridine ligands of fraction 2 are in one plane, as indicated in Figure 2b. The other H6 proton with the moderate steric interaction is observed at about 8.26 ppm. Thus, isomer **2-I** has a different orientation of the bipyridine ligands, giving no H6 doublet at about 8.4 ppm (Figures 2a and 3).

Absorption and Emission Spectra. Absorption and emission data obtained for the different compounds have been listed in Table III. The table contains data for the compounds with the deprotonated ligand bpt, as well as the protonated ligand Hbpt. The values for compounds with the protonated ligands were obtained in acidic solutions. As expected, protonation leads to a shift to higher energy for the lowest MLCT band, as indicated in Figure 5 for the mononuclear compound. Similar behavior has been observed for a series of compounds containing imidazole, pyrazole, and 1,2,4-triazole moieties and is explained by the increased π-donor capacity of the deprotonated ligand.[31,35]

By use of Figure 5, the pK_a for

$$[Ru(bpy)_2(bpt)]^+ \underset{pK_a}{\overset{+H^+}{\underset{-H^+}{\rightleftharpoons}}} [Ru(bpy)_2(Hbpt)]^{2+} \quad (1)$$

can be obtained. The value of 4.0 ± 0.1 for the pK_a is significantly lower than the value of 8.4 ± 0.1 obtained for the free ligand. So, when bound to the $Ru(bpy)_2$ moiety, the Hbpt ligand is a much

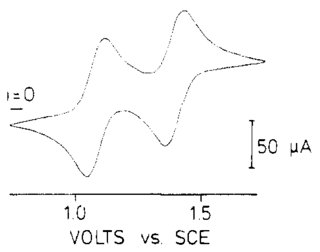

Figure 6. Cyclic voltammogram of $[(Ru(bpy)_2)_2(bpt)]^{3+}$ in 0.1 M TEAP/CH_3CN at 100 mV/s.

stronger acid than the free ligand by more than 4 orders of magnitude. This suggests substantial electron donation from the ligand to the ruthenium center. Protonation of the dinuclear compound proved to be very difficult. Experiments carried out in aqueous solution suggest a pK_a as low as -0.6 ± 0.3.

The protonations also have the expected effect on the emission spectra of mononuclear compound **1** with a shift to higher energy for the λ_{max} emission upon protonation. For protonated dinuclear compound **2** no emission was observed, probably because of quenching in acidic solutions. The data in Table III show that, surprisingly, for the dinuclear compounds the lowest MLCT band is found at higher energy than for the mononuclear compounds. This is quite in contrast with results obtained for related dinuclear systems, where this band is shifted to lower energy when compared with that of the mononuclear analogues.[14-16] Such red shifts have been explained by the stabilizing effect of the remote positive charge on the excited state. In the dinuclear compounds reported here the presence of $d\pi \rightarrow \pi^*$ transitions might be present and these might at least partly be responsible for the high energy of the MLCT band in the dinuclear compound. Interestingly, the dinuclear compound emits at room temperature and the emission maximum observed is in agreement with the differences in absorption maxima observed for mononuclear and dinuclear compounds. The emission for the dinuclear compound is found at higher energy than that for the analogous mononuclear compound.

Electrochemical Measurements. Redox properties of the mono- and dinuclear compounds are presented in Table III. $E_{1/2}$ values were determined by cyclic voltammetry. The difference in peak positions E_p ($=E_p^{ox} - E_p^{red}$) for the oxidation waves was 60–80 mV, indicating reversible electron-transfer processes.[41] The difference in oxidation potentials between the two oxidation waves of the deprotonated dinuclear compound is 0.32 V (Figure 6). This indicates either that the chemical environments of the $Ru(bpy)_2$ moieties are different (due to the different coordination modes: $N_1 + N_1'$ vs $N_1 + N_4'$) or that electrostatic interactions and/or electron delocalization are important in the dinuclear compound.[16] As shown earlier, 1-methyl-3-(pyridin-2-yl)-1,2,4-triazole binds via N4′ to the metal ion, while 4-methyl-3-(pyridin-2-yl)-1,2,4-triazole coordinates via N2′.[31,33] Nevertheless, the oxidation potentials of both $Ru(bpy)_2(LL')^{2+}$ complexes are the same. This suggests that the mode of coordination of the triazole ring does not affect the redox properties much. Therefore, the large difference in oxidation potentials of 0.32 V is most likely caused by electronic interactions between the two metal centers. This is further supported by the fact that the oxidation potential of the deprotonated mononuclear compound is slightly different from the first oxidation potential in the dinuclear compound. In general dinuclear compounds, with small electron delocalization and resonance stabilization effects, the first oxidation potential is expected to be similar to that observed for the mononuclear complexes.[17] A potential energy diagram for such a dinuclear system with a strong interaction is schematically presented in Figure 7. The difference in the two oxidation potentials in the dinuclear compound gives a quantitative measure for the comproportionation reaction[13]

$$\text{M(III)-M(III)} + \text{M(II)-M(II)} \underset{K_{com}}{\rightleftharpoons} 2\text{M(II)-M(III)} \qquad (2)$$

From

$$RT \ln K_{com} = F(\Delta E_{1/2}) \qquad (3)$$

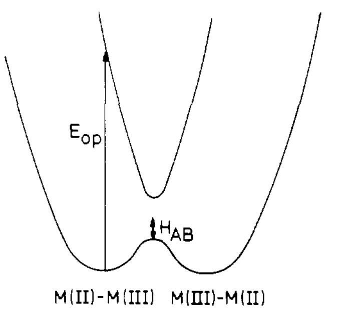

Figure 7. Potential energy versus nuclear configuration curve proposed for $[(Ru(bpy)_2)_2(bpt)]^{3+}$.

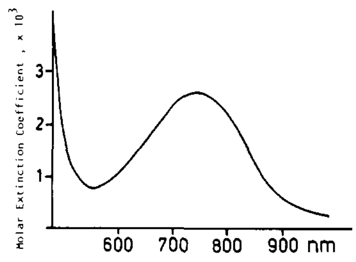

Figure 8. Intervalence transition of the mixed-valence compound $[(Ru(bpy)_2)_2(bpt)]^{4+}$, measured in acetonitrile.

a value for K_{com} of 2.4×10^5 is obtained; this value points to a rather strong interaction between the metal centers. When **2** is protonated, the two oxidation potentials shift to lower values, while the difference between the oxidation potentials becomes smaller (0.21 vs. 0.32 V). It is quite remarkable that the oxidation potentials of the protonated dinuclear compound have lower values than those of the protonated dinuclear compound because one would, for electrostatic reasons, expect that the oxidation of a species with a higher charge will occur at higher potentials.[16] The protonated dinuclear compound will most probably have a smaller extent of electron delocalization because of the higher energy of the π^* orbital. It is worth pointing out that the free ligand has two $\pi \rightarrow \pi^*$ transitions. These are found at 229 and 277 nm for the neutral ligand and at 253 and 292 nm for the deprotonated ligand. The presence of these orbitals will influence the value of the oxidation potentials as well as the difference in the two oxidation potentials of the dimer. Compared to the oxidation potentials of a series of $Ru(bpy)_2$ complexes with pyridyltriazoles, the same oxidation potential of the deprotonated monomer is observed.[31] As was mentioned above, deprotonation of the ligand leads to a stronger π-donor capacity. However, the protonated compound has a much lower oxidation potential than the ruthenium compounds with pyridyltriazoles (1.00 vs. 1.20 V). This suggests that σ-donor properties of Hbpt are stronger than those of the other pyridyltriazole ligands. This might be caused by the extra pyridine ring.

Mixed-Valence Compound. To obtain more information about the extent of electron delocalization, the deprotonated dinuclear compound was partially oxidized with $(NH_4)_2Ce(NO_3)_6$. A broad featureless band was observed at 735 nm ($\epsilon = 2600\ M^{-1}\ cm^{-1}$) with a peak width of 4340 cm^{-1} (see Figure 8). This band is assigned to an intervalence transition on basis of bandwidth, its extinction coefficient, and its solvent dependence. No absorption band at about 700 nm has been observed for the oxidized ruthenium(III) mononuclear compound. The extinction coefficient is somewhat higher than reported for related systems (typical values 50–500 $M^{-1}\ cm^{-1}$).[16,17,26,38] With use of the formula given by Hush[28]

$$\Delta\bar{\nu}_{1/2} = (2310E_{op})^{1/2}\ cm^{-1} \qquad (4)$$

where $\Delta\bar{\nu}_{1/2}$ is the bandwidth at half-intensity and E_{op} is the band maximum (λ in cm^{-1}), a value of $\Delta\bar{\nu}_{1/2} = 5.6 \times 10^3\ cm^{-1}$ is found. This value is higher than the value observed for $\Delta\bar{\nu}_{1/2}$ and suggests that this species might be an example of a class III mixed-valence compound or that at least interaction between the centers is

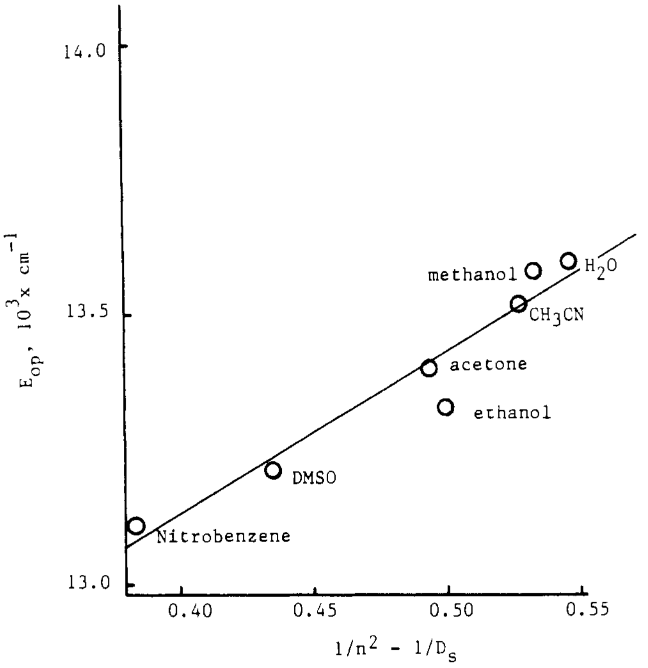

Figure 9. Solvent dependency of the intervalence-transition band energies of $[(Ru(bpy)_2)_2(bpt)]^{4+}$.

strong.[41] The extent of electron delocalization can be calculated from eq 5, by using the extinction coefficient of the IT band (ϵ

$$\alpha^2 = (4.2 \times 10^{-4})\epsilon(\Delta\bar{\nu}_{1/2})/d^2E_{op} \qquad (5)$$

in M^{-1} cm^{-1}), the distance between the ruthenium centers (d in Å), E_{op} (in cm^{-1}), and $\Delta\bar{\nu}_{1/2}$ (in cm^{-1}). d was estimated to be 6.1 Å, by using the Ru–N distances of $[Ru(bpy)_3]X_2$[43] and the X-ray structure of $[Cu_2(H_2O)_2(CF_3SO_3)_2(bpt)_2]$.[44] In this manner a value for α^2 of 9.4×10^{-3} was obtained for this compound. This value for α^2 is higher then reported in literature for similar systems.[21-29] It can be concluded therefore that the large difference in oxidation potentials of this compound is probably caused by the rather high extent of electron delocalization.

The magnitude of the electronic coupling can be calculated by using eq 6,[28,41] where H_{ab} is the magnitude of electronic coupling

$$H_{ab} = 2.05 \times 10^{-2}\left[\frac{\epsilon_{max}(\Delta\bar{\nu}_{1/2})}{E_{op}}\right]^{1/2}\frac{E_{op}}{d}\ cm^{-1} \qquad (6)$$

(see Figure 7); ϵ_{max}, $\Delta\bar{\nu}_{1/2}$, E_{op}, and d have been explained previously (see eq 4 and 6 for further details). The value calculated for H_{ab} here is 1340 cm^{-1}, which is, compared to values found in other systems, quite high.[41]

A plot of the energy of the intervalence-transfer band of the mixed-valence compound as a function of the solvent is shown in Figure 9. The value of the slope is 2969 cm^{-1}, and the intercept is 11940 cm^{-1}. For this compound, the slope obtained is smaller than in most other systems.[41,42]

According to Hush, the position of the intervalence transition is dependent on the intramolecular (χ_s) energies:[28]

$$E_{op} = \chi_i + \chi_s \qquad (7)$$

χ_s is, according to the dielectric continuum theory, dependent on the dielectric properties of the medium:[28]

$$\chi_s = e^2(1/r - 1/d)(1/n^2 - 1/D_s) \qquad (8)$$

In eq 8, e is the unit electronic charge, r is the molecular radius of the redox sites, d is the separation between the ruthenium ions, and n^2 and D_s are the optical and static dielectric constants of the solvent. From eq 8, a value of $\delta E_{op}/\delta(1/n^2 - 1/D_s) = 1220$ cm^{-1} was calculated, which is 40% of the observed value of the slope (3100 cm^{-1}). Such discrepancies have also been observed for other dinuclear complexes with a short metal–metal distance.[23,25,41]

Qualitatively, the slope should increase with the metal–metal distance (r), as is observed for a series of ruthenium dinuclear compounds with various bridging ligands.[41] Therefore, because of the small distance between the redox sites, the solvent dependency is quite small for this system. The slope observed might also be explained by assuming that a certain extent of electron delocalization in the Ru^{II}–Ru^{III} compound is present.[25] This is in agreement with the large difference in the oxidation potentials of the dinuclear ruthenium compound, the high value obtained for α^2, and the rather narrow bandwidth of the intervalence transition.

Concluding Remarks. The results discussed above have made clear that bpt is a very interesting bridging ligand. We have been able for the first time to separate two sets of isomers by recrystallization techniques. The NMR data reported in this work show clearly the importance of this technique in the study of the different isomers.

In its deprotonated form the bridging ligand mediates a rather strong interaction between the ruthenium centers. This strong electron delocalization is most likely facilitated by the low π^* orbital in the bridging ligand and also by the presence of a negative charge on the bridging triazole ring. From the spectroscopic and electrochemical evidence, the dinuclear ruthenium compound can be classified as a class II material with strong interaction between the sites, possibly on the class II/class III borderline. The dinuclear compound containing the protonated ligand is much more difficult to investigate, as protonation occurs only at very low pH, but electrochemical evidence suggests that interaction between the metal centers is reduced compared to that of the deprotonated dinuclear compound. This is most likely caused by the shift in π^* orbital and the absence of the negative charge on the bridging triazole ring.

The decrease in pK_a values obtained for both the mononuclear and dinuclear compound suggests a strong electron donation from the bpt ligand to the ruthenium center. The increased delocalization of the charge in the dinuclear compound is most likely responsible for the difference in acidity of about 10 orders of magnitude between the dinuclear ruthenium compound and the free ligand.

No differences in the electronic and electrochemical properties between the two isolated isomers are observed.

Acknowledgment. We gratefully acknowledge the interest in the electrochemical measurements of Dr. J. G. M. van der Linden and H. Blonk of the University of Nijmegen, The Netherlands. We also thank A. W. M. Lefeber and C. Erkelens for their help in recording the NMR spectra. Furthermore, we wisk to thank Johnson and Matthey Chemicals Ltd. (Reading, UK) for their generous loan of $RuCl_3$.

Registry No. $[Ru(bpy)_2(bpt)](PF_6)$, 114397-52-3; $Ru(bpy)_2Cl_2$, 19542-80-4; $[(Ru(bpy)_2)_2(bpt)](PF_6)_3$ (isomer **2-I**), 114397-54-5; $[(Ru(bpy)_2)_2(bpt)](PF_6)_3$ (isomer **2-II**), 114488-39-0; $[Ru(bpy)_2(Hbpt)]^{2+}$, 114397-55-6; $[(Ru(bpy)_2)_2(Hbpt)]^{4+}$ (isomer **2-I**), 114397-56-7; $[(Ru(bpy)_2)_2(Hbpt)]^{4+}$ (isomer **2-II**), 114488-40-3; $[(Ru(bpy)_2)_2(bpt)]^{4+}$, 114397-57-8; $[(Ru(bpy)_2)_2(bpt)]^{5+}$, 114397-58-9.

---

(43) Rillema, D. P.; Jones, D. S.; Levy, H. A. *J. Chem. Soc., Chem. Commun.* **1979**, 849.
(44) Prins, R.; Birker, P. J. M. W. L.; Haasnoot, J. G.; Verschoor, G. C.; Reedijk, J. R. *Inorg. Chem.* **1985**, *24*, 4129.